Frequency-Dependent Modeling of Power Transformers With Ungrounded Windings

Bjørn Gustavsen, *Senior Member, IEEE*

***Abstract*—A linear wideband transformer model for the purpose of simulation of electromagnetic (EM) transients has previously been developed by the author. The model was obtained via frequency-domain measurements and rational approximation of the terminal admittance matrix Y. In the case of transformers with ungrounded windings, the model may produce erroneous results due to a near singular condition at low frequencies. This paper shows that the problem can be overcome by explicit measurement and modeling of the zero sequence system. Blocks of Y, which correspond to ungrounded windings, are modified by removal of their zero sequence components. A new zero sequence system is obtained by dedicated measurements and the two functions are approximated with rational functions which are combined to produce the final model. Application to a wye-delta-connected transformer demonstrates the validity of the approach.**

***Index Terms*—Electromagnetic transients, EMTP, frequency dependence, measurement, power transformer, simulation.**

I. Introduction

HIGH-frequency transformer models are useful in studies of transferred overvoltages between voltage levels and resonant overvoltage situations involving transformers. A suitable type of transformer model is the terminal equivalent [1], [2], which models the voltage/current characteristics at the transformer terminals.

In a previous paper [3], the author has described the measurement procedure and modeling technique used for obtaining a wideband linear terminal equivalent of power transformers with grounded windings. The model was obtained by measuring the admittance matrix Y in the frequency domain using a network analyzer. Y was next partitioned into blocks according to its windings, and each block was subjected to rational approximation with a common set of poles. The rational approximations were finally combined to give the transformer model.

The previous model may, however, produce erroneous results at low frequencies for transformers with ungrounded windings because the (capacitive) coupling to ground of an ungrounded winding approaches zero with decreasing frequency, thereby causing a near singular condition for the associated block in Y.

This paper presents a solution to this problem by removing the zero sequence system from the blocks of Y which correspond to ungrounded windings. A new zero sequence system is obtained by dedicated measurements and the two admittances are approximated by rational functions and combined into the final model. The procedure is demonstrated for a wye-delta-connected transformer and the resulting model is validated by comparison with recorded waveforms.

Manuscript received January 2, 2003. This work was supported by the European Commission under the Fifth Frame Programme by a DG Research Non Nuclear Energy Programme Marie Curie Fellowship.

The author is with SINTEF Energy Research, Trondheim N-7465, Norway (e-mail: bjorn.gustavsen@sintef.no).

Digital Object Identifier 10.1109/TPWRD.2004.824381

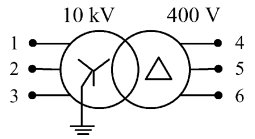

Fig. 1. Transformer with ungrounded low-voltage winding.

II. Transformer With Ungrounded Windings

A two-winding transformer is considered with windings denoted H (high voltage) and L (low voltage), respectively. This gives in the frequency domain a short-circuit admittance matrix of the form

$$\begin{bmatrix} I_H \\ I_L \end{bmatrix} = \begin{bmatrix} Y_{HH} & Y_{HL} \\ Y_{LH} & Y_{LL} \end{bmatrix} \cdot \begin{bmatrix} V_H \\ V_L \end{bmatrix} \tag{1}$$

where the blocks (submatrices) are of size 3×3. All quantities in (1) are functions of frequency s. The elements of (1) can be measured directly in the phase domain (e.g., by using the measurement setup described in [3]).

In general, the diagonal elements of the blocks in (1) become large at low frequencies as the short-circuit currents increase due to the decrease in impedances sL. At the same time, the zero-sequence component of diagonal and offdiagonal blocks associated with ungrounded windings becomes very small because the only connection to ground is via capacitors. This causes these blocks to get one small eigenvalue and two large eigenvalues, implying matrices with a high condition number. As was explained in [3], a matrix with a high condition number is very sensitive to perturbations of the data and, thus, to measurement errors.

The following example demonstrates that an ungrounded winding can cause the transformer model to produce highly incorrect results. Fig. 1 shows the same two-winding transformer as used for the examples in [3], but with the secondary reconnected into delta.

Fig. 2 shows the eigenvalues of Y_{LL} of the measured admittance matrix. The inherently low accuracy of the measurements (e.g., 1%) results in that the contribution from the smallest eigenvalue tends to become lost in the measured responses. The calculated eigenvalue (trace 3) therefore becomes highly inaccurate at low frequencies where it is seen to increase with decreasing frequency, instead of decreasing. Also shown is the

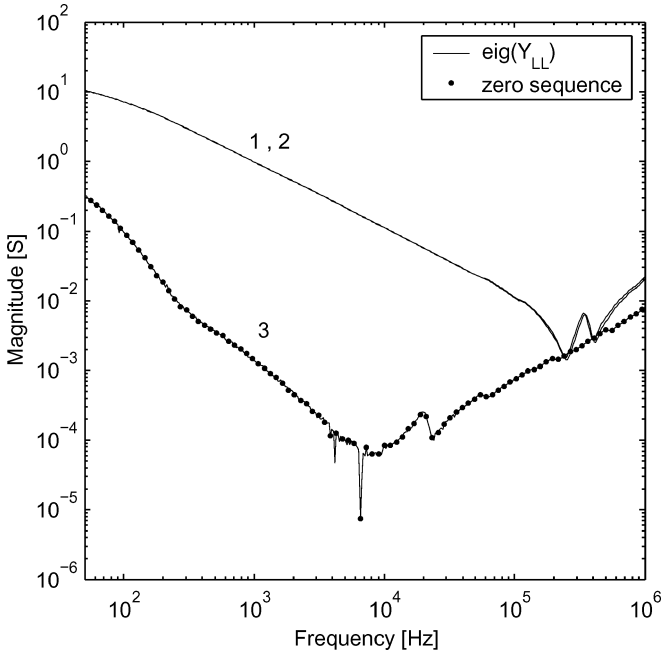

Fig. 2. Eigenvalues of Y_{LL}.

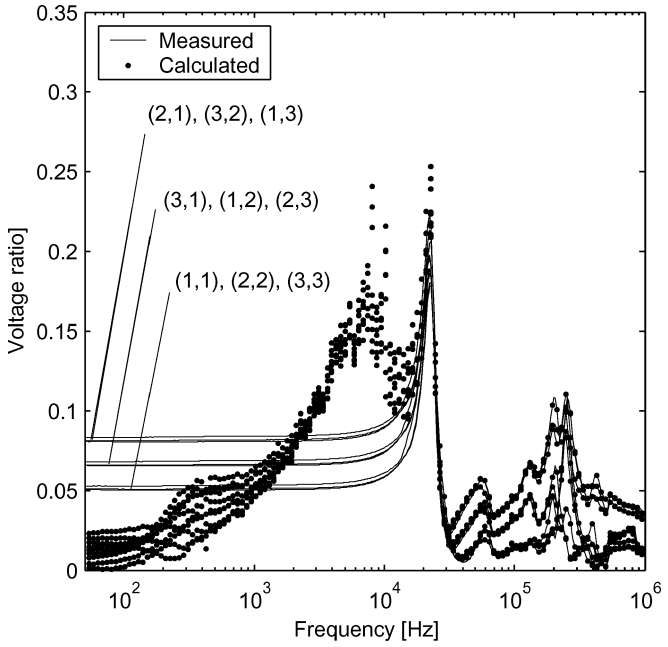

Fig. 3. Measured and calculated elements of V_{LH}.

zero sequence component of Y_{LL} (the sum of all matrix elements divided by 3) which can be seen to closely match the smallest eigenvalue. A similar result was also found for Y_{HL} and Y_{LH}.

Fig. 3 compares the measured voltage ratio from high to low with the voltage ratio as calculated from the expression [3]

$$V_{LH} = -Y_{LL}^{-1} Y_{LH}. \tag{2}$$

It is seen that the calculated voltage is highly incorrect at frequencies below 20 kHz. This result occurs because the smallest eigenvalue in Y_{LL} and in Y_{LH} are inaccurate.

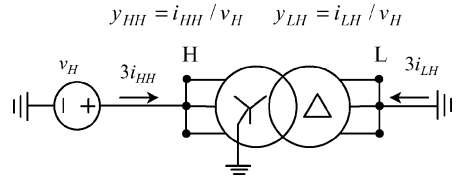

Fig. 4. Zero-sequence measurement.

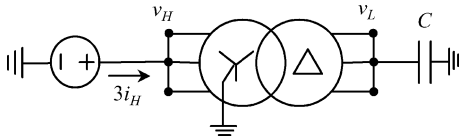

Fig. 5. Adding capacitor to ungrounded winding.

III. Zero Sequence Measurements

The result in Fig. 2 showed that the smallest eigenvalue of Y_{LL} closely corresponds to the zero sequence component. Thus, the accuracy problem can be overcome by replacing the zero sequence component with one obtained by a more accurate measurement.

For the two-winding transformer, we have a 2×2 zero sequence admittance matrix Y_0

$$Y_0 = \begin{bmatrix} y_{HH} & y_{HL} \\ y_{LH} & y_{LL} \end{bmatrix}. \tag{3}$$

The elements of Y_0 can be measured directly by treating each winding as a single terminal. The procedure is shown in Fig. 4 for the measurement of y_{HH} and y_{LH}.

However, it was found that the elements associated with the ungrounded winding (y_{HL}, y_{LH}, y_{LL}) became highly inaccurate at very low frequencies because the current was too small to be accurately measured. This problem was overcome by using an indirect measurement procedure based on the change in the measured voltage ratio when adding a capacitor to the open terminal (see Fig. 5).

After connecting the capacitor, the 2×2 zero sequence admittance matrix becomes

$$\begin{bmatrix} i_H \\ i_L \end{bmatrix} = \begin{bmatrix} y_{HH} & y_{HL} \\ y_{LH} & y_{LL} + \frac{j\omega C}{3} \end{bmatrix} \cdot \begin{bmatrix} v_H \\ v_L \end{bmatrix}. \tag{4}$$

With the low-voltage terminal open ($i_L = 0$), the voltage ratio from high to low can be obtained from the second equation in (4). The voltage ratio, before and after introduction of the capacitor, becomes

$$v_{LH} = -\frac{y_{LH}}{y_{LL}} \tag{5}$$

$$\hat{v}_{LH} = -\frac{y_{LH}}{\left(y_{LL} + \frac{j\omega C}{3}\right)}. \tag{6}$$

Combining (5) and (6) to eliminate y_{LL} gives

$$y_{LH} = \frac{-j\omega C \cdot \hat{v}_{LH}}{3\left(1 - \frac{\hat{v}_{LH}}{v_{LL}}\right)}. \tag{7}$$

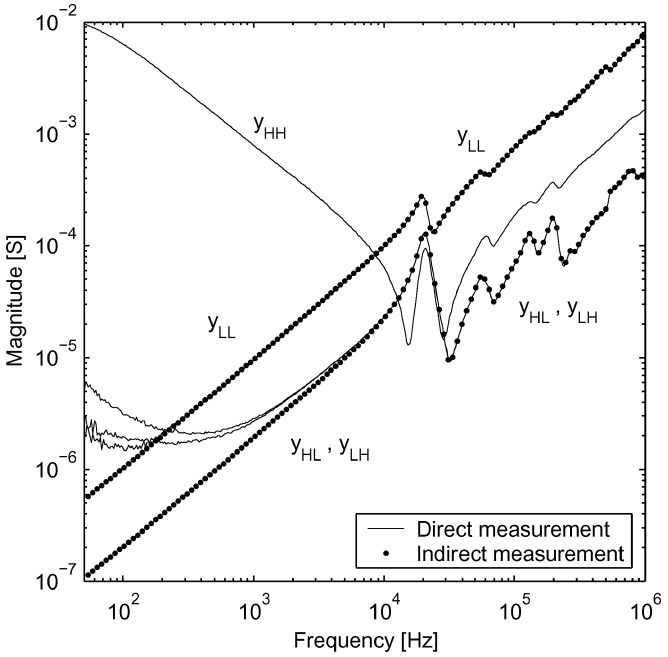

Fig. 6. Admittance of zero-sequence system.

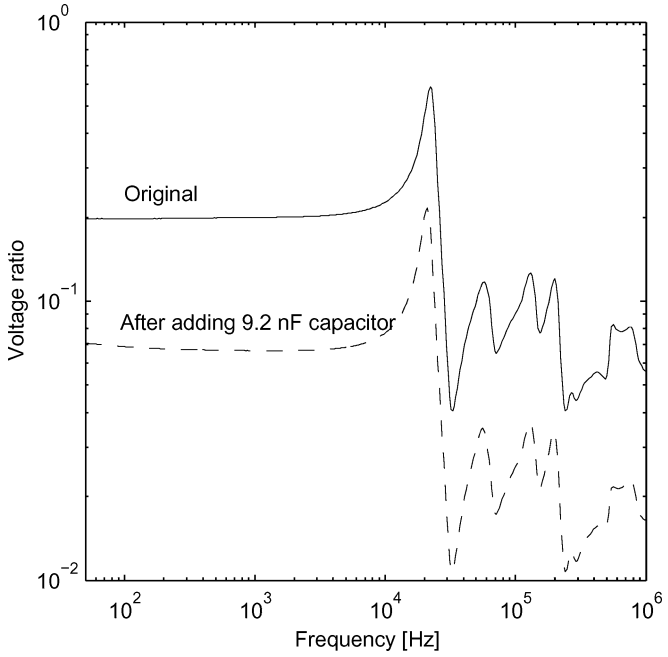

Fig. 7. Effect of capacitor on measured voltage ratio v_{LH}.

The phase domain blocks Y_{HL} and Y_{LH} are symmetric with respect to each other, implying

$$y_{HL} = y_{LH}. \tag{8}$$

From (5), we get

$$y_{LL} = -\frac{y_{LH}}{v_{LH}}. \tag{9}$$

Fig. 6 compares the elements of Y_0 when measured directly and when measured indirectly using (7)–(9) with a 9.2-nF capacitor. It is seen that the methods give virtually the same results at high frequencies. At low frequencies, however, the indirect method gives the desired capacitive behavior for elements y_{HL}, y_{LH}, y_{LL} whereas the direct method produces an incorrect result.

The size of the capacitor has to be chosen so that a significant change results in the voltage ratio, for all frequencies. Fig. 7 shows the open-circuit voltage ratio, before and after adding the 9.2-nF capacitor.

IV. Modification of Admittance Matrix

The introduction of the zero sequence system is done separately for each matrix block that needs to be corrected (i.e., Y_{HL}, Y_{LH}, Y_{LL}). This is achieved by the following three steps:

1) Subtract from each row, the average value of the row.
2) Subtract from each column, the average value of the column.
3) Add to all elements of the block the measured zero-sequence admittance divided by 3.

The first step has the effect that the block gets one zero eigenvalue with eigenvector equal to $[1\ 1\ 1]^{\mathrm{T}}$, thus being a zero sequence eigenvalue with zero value. The second step has the effect that the two other eigenvectors become orthogonal to the zero sequence eigenvector (without changing the eigenvalues).

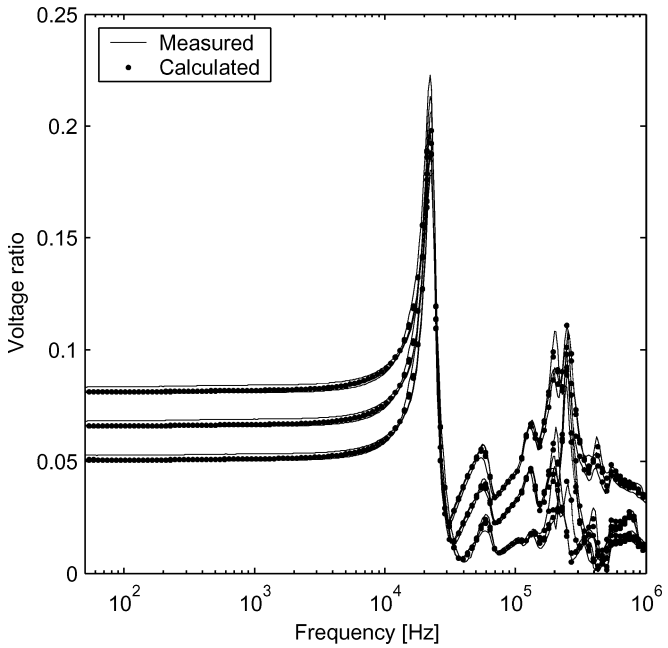

Fig. 8. Effect of modification on V_{LH}.

The third step introduces the measured zero sequence component into the block.

Fig. 8 shows the effect of this approach on V_{LH}. Comparison with Fig. 3 shows that the erratic behavior at low frequencies has been removed.

V. Modeling

The modified Y can, in principle, be subjected to rational approximation using the same procedure as was described in [3]. However, the inevitable fitting errors contain a zero sequence component which would cause large errors at low frequencies,

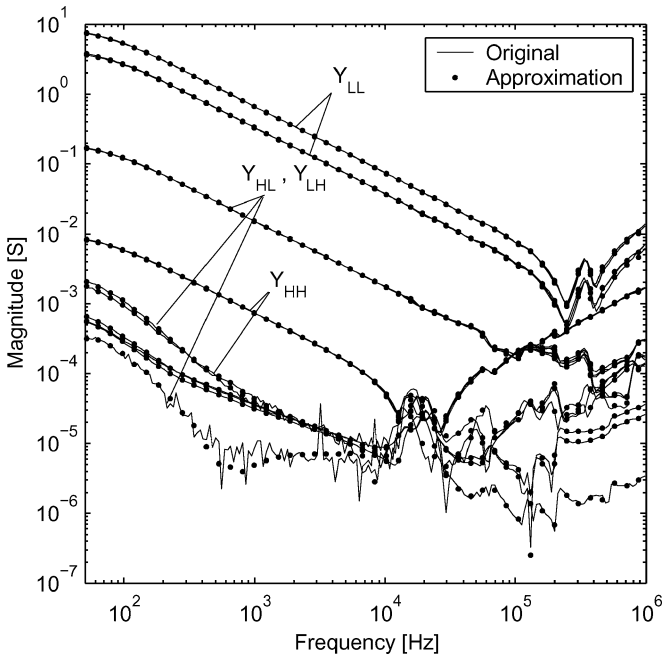

Fig. 9. Rational approximation of modified Y.

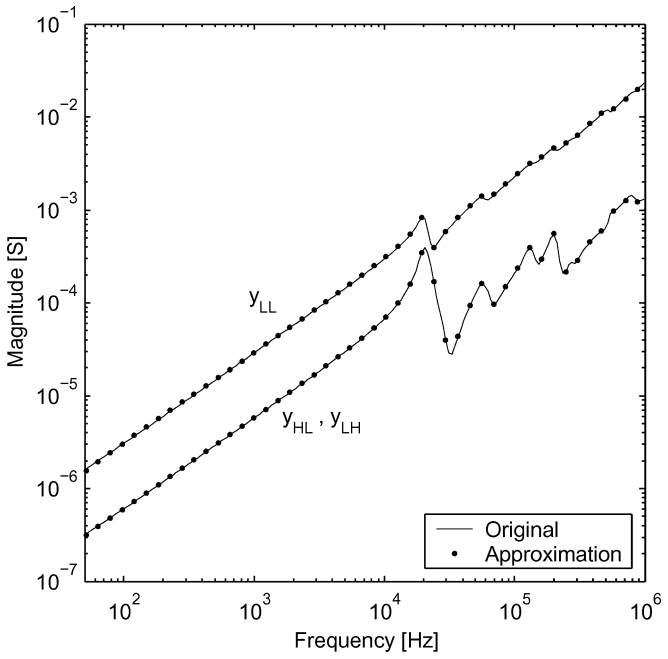

Fig. 10. Rational approximation of measured zero sequence system.

similarly as in Fig. 3. This difficulty was overcome using the following procedure:

1) Remove from relevant blocks of the measured Y, the zero sequence component.
2) Subject the modified Y to rational approximation.
3) Remove from relevant blocks of the rational approximation, the zero sequence component.
4) Subject the measured zero sequence admittance Y_0 to rational approximation.
5) Combine the rational approximation of Y_0 with the one of the modified Y

The following deliberates on the details with basis in the previous example.

Step 1) The zero sequence system is removed for blocks Y_{HL}, Y_{LH}, and Y_{LL} using steps 1 and 2 described in Section IV.

Step 2) Each block of the modified Y is subjected to rational function approximation using a common set of poles. Fig. 9 shows the rational approximation of the modified Y, as fitted using 50 poles per column for each block. It is seen that high accuracy has been achieved.

Step 3) The fitting errors will produce a zero sequence component which has to be removed. This is achieved by considering that each block of the modified Y has been fitted by a common set of poles, that is

$$Y_{\rm mod} = \sum_{m=1}^{N} R_m \frac{1}{s - a_m} + D + sE. \qquad (10)$$

The removal of the zero sequence is done by applying to R_m, D, and E steps 1-2 described in Section IV. This results in that each of these matrices gets a zero sequence eigenvalue with zero value, with associated eigenvector being orthogonal to the other eigenvectors.

Step 4) Fig. 10 shows the elements of the measured zero sequence system Y_0 as fitted with a common set of 30 poles. Note that element y_{HH} has been omitted because block Y_{HH} does not need to be corrected.

Step 5) The rational approximations of $Y_{\rm mod}$ and Y_0 are next combined into a single realization. Each block of Y gets an approximation as shown in (11), where the second term is the contribution from the zero sequence system. U is a 3×3 matrix whose elements are equal to 1/3. The two terms in (11) are finally combined into a realization of the form (*A*, *B*, *C*, *D*, *E*)

$$Y_{\rm sub} = Y_{\rm mod} + U\left(\sum_{m=1}^{N_0} \frac{r_{0,m}}{s - a_m} + d_0 + se_0\right). \qquad (11)$$

Fig. 11 shows the accuracy of the resulting approximation of Y. Comparison with Fig. 9 shows that the accuracy has deteriorated somewhat for the smallest elements.

Figs. 12 and 13 compare the measured voltage ratio V_{LH} and V_{HL} with the corresponding quantities calculated from the rational approximation. It can be seen that the rational approximation reproduces the measured voltage ratio V_{HL} with a high degree of accuracy. The accuracy of V_{LH} is somewhat lower.

VI. Time-Domain Results

A series of time-domain measurements and corresponding simulations have been carried out in order to verify the accuracy of the resulting model. All time-domain measurements were made directly on the transformer terminals. The capacitive effect of the 1-m-long measurement cables was taken into account by modifying the diagonal elements, as described in [3]. All

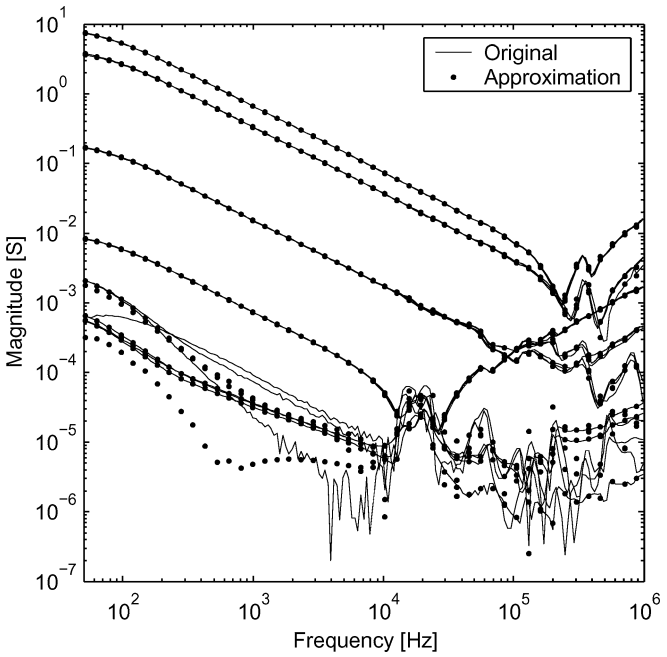

Fig. 11. Resulting approximation of Y.

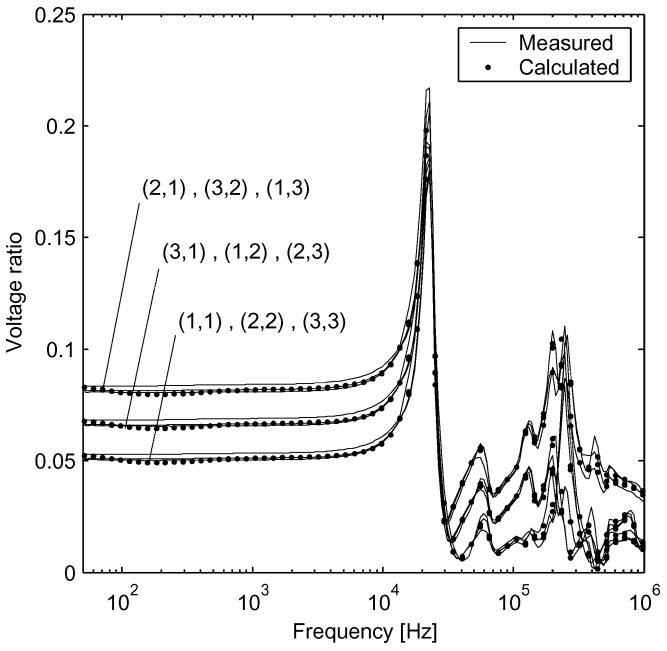

Fig. 12. Voltage ratio V_{LH}.

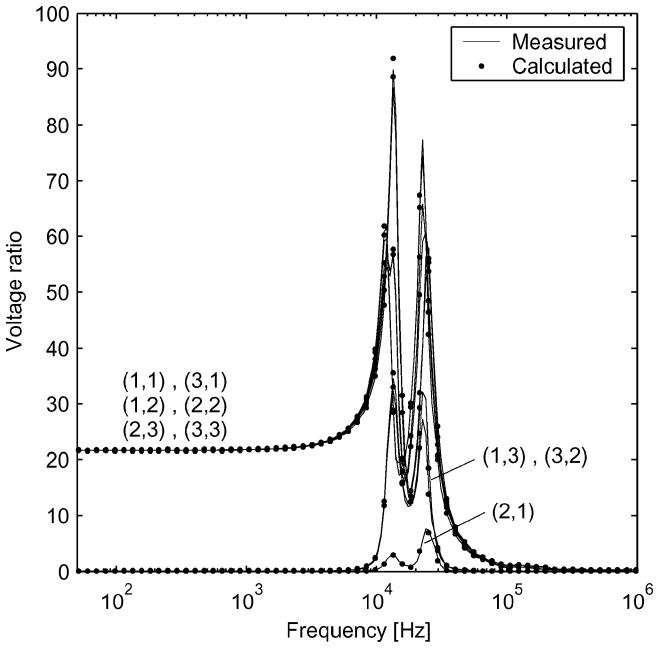

Fig. 13. Voltage ratio V_{HL}.

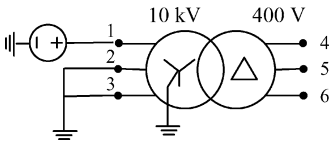

Fig. 14. Excitation on high-voltage side.

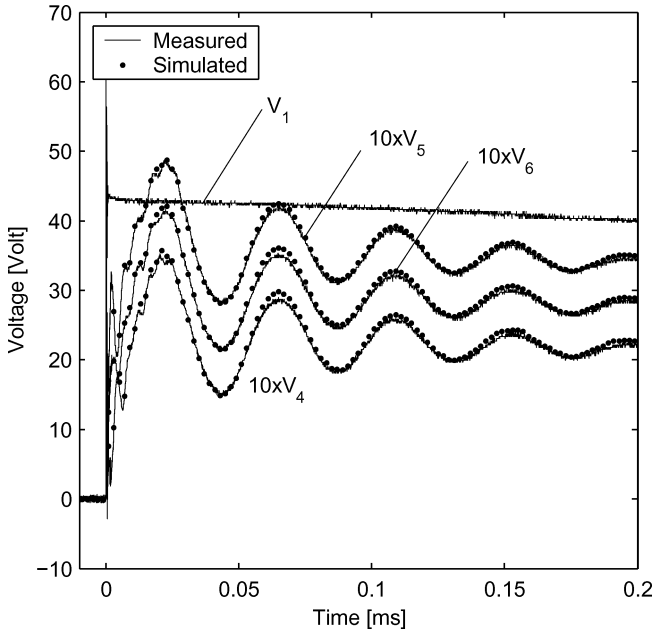

Fig. 15. Voltage response on low-voltage side.

calculations were done using MatTran [4] with the transformer model implemented as a user-defined subroutine.

Fig. 14 shows a test where terminal 1 on the high-voltage side is energized by a steep fronted voltage impulse. A simulation for this case was carried out where the measured voltage on terminal 1 was taken as an ideal voltage source. Fig. 15 compares the measured and simulated wave forms on terminals 4,5,6 on the low-voltage side. It is seen that the model reproduces the measured waveforms with a high degree of accuracy.

Any external network can be connected to the transformer. Fig. 16 shows an example where 6.8-nF capacitors are connected to the low-voltage terminals and 412-Ω resistors are connected to the high-voltage terminals. This approximately represents the situation of an incoming surge on a connected overhead line on the high-voltage side. The capacitors will approximately represent a cable stub of about 20 m. Fig. 17 compares measured and simulated waveforms on terminals 2,4,6 when applying a near step voltage on terminal 7. The voltage on ter-

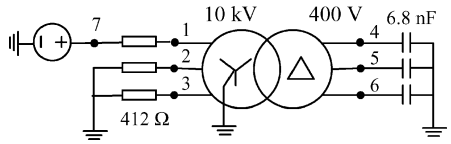

Fig. 16. Transformer connected to external circuit.

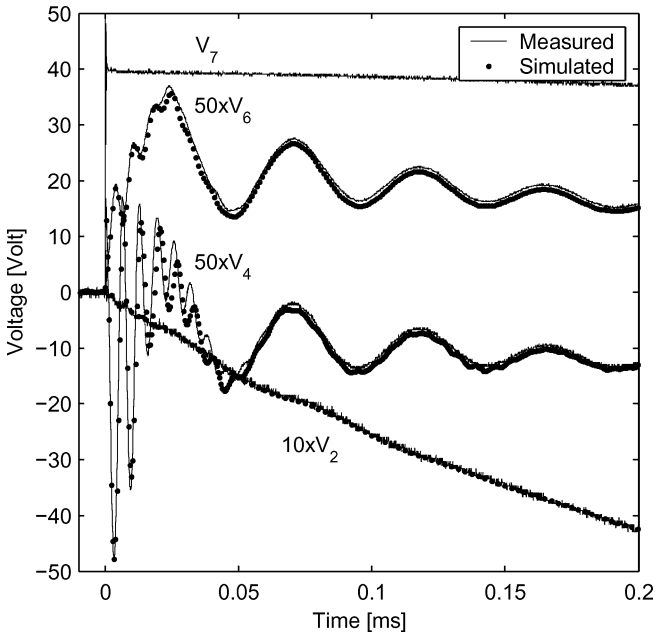

Fig. 17. Voltage responses.

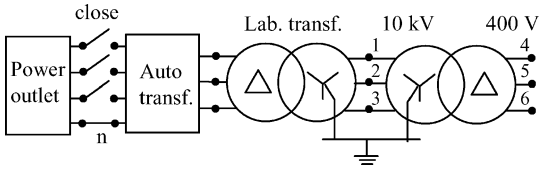

Fig. 18. Energization from 50-Hz power source.

minal 7 was taken as a known voltage in the simulation. Again, a good agreement between measured and simulated waveforms has been achieved.

Fig. 18 shows an example where the transformer is energized from a three-phase power source. The measured voltages on terminals 1,2,3 are taken as known voltage sources in the simulation. Fig. 19 compares the measured and simulated waveform on terminal 4. It can be seen that the 50-Hz component has been correctly reproduced.

Fig. 20 shows an example of impulse voltage energization on the low-voltage side. The results in Fig. 21 verify that the model also produces the correct result for the voltages on the high-voltage side.

VII. Conclusion

This paper has described a procedure for the modeling of transformers with ungrounded windings, based on measured frequency responses. Ungrounded windings need special treatment because the zero sequence system can become highly inaccurate when the modeling is based on phase-domain measurements. The difficulty was overcome as follows.

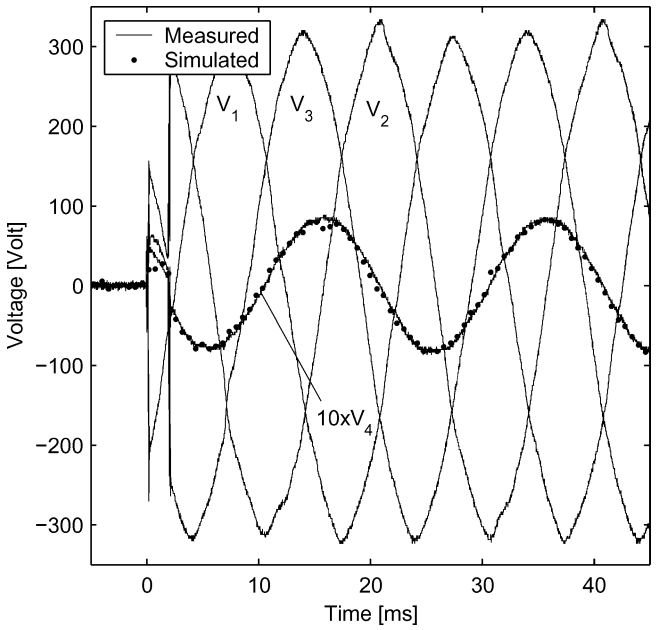

Fig. 19. Measured and simulated waveforms.

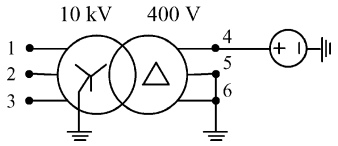

Fig. 20. Excitation on low-voltage side.

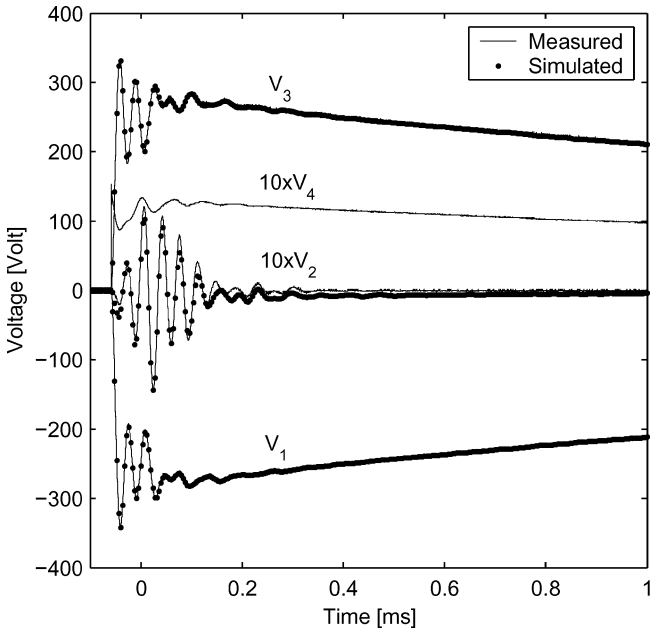

Fig. 21. Voltage response on high-voltage side.

1) The measured transformer admittance matrix Y is partitioned into blocks according to its windings.
2) Blocks associated with an ungrounded winding are modified by removal of their zero sequence component, and by enforcing their remaining eigenvectors to be orthogonal to that of the zero sequence component.

3) The zero sequence component of these blocks is measured explicitly in the frequency domain. A measurement procedure based on voltage ratios is used in order to increase the accuracy at low frequencies.
4) A rational approximation is calculated for the modified Y. The parameters of the approximation are adjusted for the blocks associated with ungrounded windings in order to preserve the properties listed under point 2.
5) A rational approximation is calculated for the measured zero sequence components.
6) The rational approximation of the modified Y and the zero sequence components is combined into the final model.

Application to a two-winding transformer in wye-delta configuration has demonstrated the validity of the approach. The model was shown to accurately reproduce measured time-domain waveforms when the transformer was energized by an impulse voltage generator and by a three-phase 50-Hz source.

ACKNOWLEDGMENT

The author expresses his thanks to Prof. K. Feser and the staff at the Institut für Energieübertragung und Hochspannungstechnik, University of Stuttgart, Germany, for providing laboratory facilities and support of this project.

REFERENCES

[1] A. Morched, L. Marti, and J. Ottevangers, "A high frequency transformer model for the EMTP," *IEEE Trans. Power Delivery*, vol. 8, pp. 1615–1626, July 1993.
[2] B. Gustavsen and A. Semlyen, "Application of vector fitting to the state equation representation of transformers for simulation of electromagnetic transients," *IEEE Trans. Power Delivery*, vol. 13, pp. 834–842, July 1998.
[3] B. Gustavsen, "Wide band modeling of power transformers," *IEEE Trans. Power Delivery*, vol. 19, pp. 414–422, Jan. 2004.
[4] J. Mahseredjian and F. Alvarado, "Creating an electromagnetic transients program in Matlab: MatEMTP," *IEEE Trans. Power Delivery*, vol. 12, pp. 380–388, Jan. 1997.

Bjørn Gustavsen (M'94–SM'03) was born in Harstad, Norway, in 1965. He received the M.Sc. and Dr.-Ing. degrees in 1989 and 1993, respectively, from the Norwegian Institute of Technology, Trondheim.

Currently, he is with SINTEF Energy Research, Trondheim. He spent 1996 as a Visiting Researcher at the University of Toronto, ON, Canada, and the summer of 1998 at the Manitoba HVDC Research Centre, Winnipeg, MB, Canada. He was a Marie Curie Fellow at the University of Stuttgart, Germany, from August 2001 to August 2002. His interests include simulation of electromagnetic transients and modeling of frequency-dependent effects.